CZMIL (Coastal Zone Mapping and Imaging Lidar) Bathymetric Performance in Diverse Littoral Zones

Vinod Ramnath, Viktor Feygels, Hemanth Kalluri, Brant Smith
Teledyne Optech, Inc.
Kiln, USA
vinod.ramnath@teledyneoptech.com

Abstract—**The Coastal Zone Mapping and Imaging Lidar system (CZMIL) is an integrated lidar-imagery sensor system, and its complementary HydroFusion software suite is designed for the highly automated generation of physical and environmental information products for mapping the coastal zone. CZMIL is designed to survey over a wide range of water types, ranging from moderately clear to predominantly turbid. In this paper, we will discuss CZMIL's performance over a broad spectrum of environmental conditions. We will demonstrate that high-power laser systems with wide-aperture optics are key to optimum performance in turbid water conditions. We will also discuss the challenges with objective measurement of turbid water optical properties. Finally, we will discuss the small-object detection capability of CZMIL and show how post-processing software enhances the hardware's detection capability.**

Keywords—lidar, bathymetry, coastal zone, CZMIL, water turbidity, diffuse attenuation coefficient, Aqua MODIS

I. Introduction

The Coastal Zone Mapping and Imaging Lidar (CZMIL) is an airborne multi-sensor system that exploits the data fusion paradigm to generate automated and high-resolution 3D environmental maps of coastal zones. Combined with its complementary HydroFusion data processing software suite, CZMIL offers a comprehensive list of advanced products including water characterization maps, benthic classification maps, and coastal management products like shoreline extraction vectors and dune heights. CZMIL, compared to earlier lidar systems, is an evolution of lidar bathymetric technology in terms of coastal zone mapping and monitoring beyond hydrographic surveying [1].

The lidar is a hybrid scanned-flash system employing a 10-kHz laser and circular scanner, with a segmented detector enabling simultaneous recording of high-density topo/bathy data from a single laser. CZMIL's high-power laser with a short pulse width addresses the combination of energy and pulse characteristics required for surveying in shallow turbid water. These design factors produce high-resolution maps in shallow water without compromising detection in deeper waters. The spectrometer (ITRES CASI-1500H) is pointed to nadir and functions as a push-broom imager. The camera, T-4800, is a 16-Megapixel frame camera, also pointed to nadir, and operates with a frame rate sufficient to achieve the desired minimum forward overlap of 25% [1].

A schematic of CZMIL in operation is shown in Fig. 1. CZMIL's technical characteristics are summarized in TABLE I.

CZMIL was designed by Teledyne Optech for the Joint Airborne Lidar Bathymetry Technical Center of Expertise (JALBTCX) to meet the requirements of the USACE National Coastal Mapping Program [2]. CZMIL was first deployed by JALBTCX in the summer of 2012 and has been in operation since then. To make this technology available and feasible to agencies worldwide, without incurring the acquisition cost of a new system, Teledyne Optech launched the CZMIL Project Program in the summer of 2014 [3].

CZMIL's hardware and HydroFusion software underwent several refinements in the past year. CZMIL Nova is a lighter and more compact redesign of the system hardware with lower power consumption, offering more system reliability and more versatile platform integration for smaller and more economically efficient aircraft. CZMIL Nova's installation layout is illustrated in Fig. 2. The Piper Navajo aircraft used in one of the surveys and the CZMIL installation on board are shown in Fig. 3.

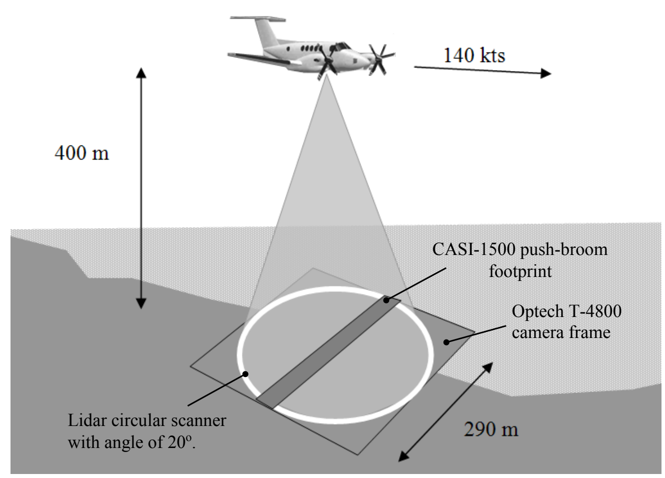

Fig. 1. Illustration of CZMIL in operation.

TABLE I. CZMIL NOVA SPECIFICATIONS

	Parameter	Specification
General	Operating altitude	400 m (nominal) up to 1,000 m
	Aircraft speed	140 kts (nominal)
	Hyperspectral sensor	CASI-1500H
	Digital cameras	Optech 16-Mpixel or 80-Mpixel camera
	Positioning and attitude	Applanix POS/AV 5.0 GPS and GLONASS
Lidar Hydrographic Mode	Shallow channels measurement rate	70 kHz
	Shallow channels maximum depth	$2/K_d$ (bottom reflectivity > 15%, K_d is the diffuse attenuation coefficient)
	Deep channel measurement rate	10 kHz
	Deep channel maximum depth	$4.2/K_d$ (bottom reflectivity > 15%)
	Horizontal measurement accuracy	(3.5 + 0.05 depth) m, 2σ
	Depth measurement accuracy	$\sqrt{}(0.32+(0.013\ \text{depth})^2)$ m, 2σ
	Scan angle	20° circular
Lidar Topographic Mode	Measurement rate	80 kHz
	Horizontal measurement accuracy	±1 m, 2σ
	Vertical measurement accuracy	±15 cm, 2σ
Physical	Power requirements	85A @ 28 VDC for lidar/camera 95A @ 28 VDC with CASI – 1500H
	Operating temperature	0°C to 40°C
	Storage temperature	-10°C to +60°C

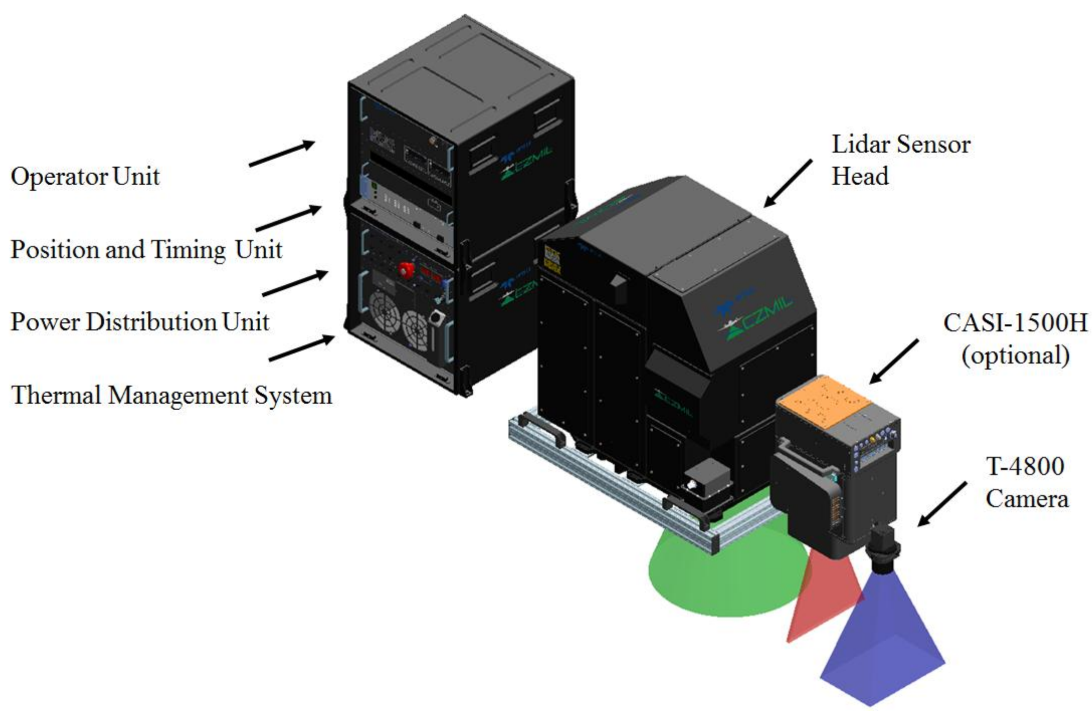

Fig. 2. CZMIL Nova installation layout

(a) (b)

Fig. 3. Piper Navajo aircraft (a) with CZMIL installed inside (b).

This paper presents CZMIL's performance in several survey locations over the last three years from its first deployment in 2012. The survey areas cover a broad spectrum of water turbidity – from clear water to turbid water conditions. Apart from the production surveys along the US coast, several survey missions were carried out over the Asia-Pacific region and the clear waters of Hawaii. In this paper, we discuss some of these surveys, whose areas of interests are shown in Fig. 4. These surveys were conducted by JALBTCX and through the CZMIL Project Program using CZMIL and CZMIL Nova.

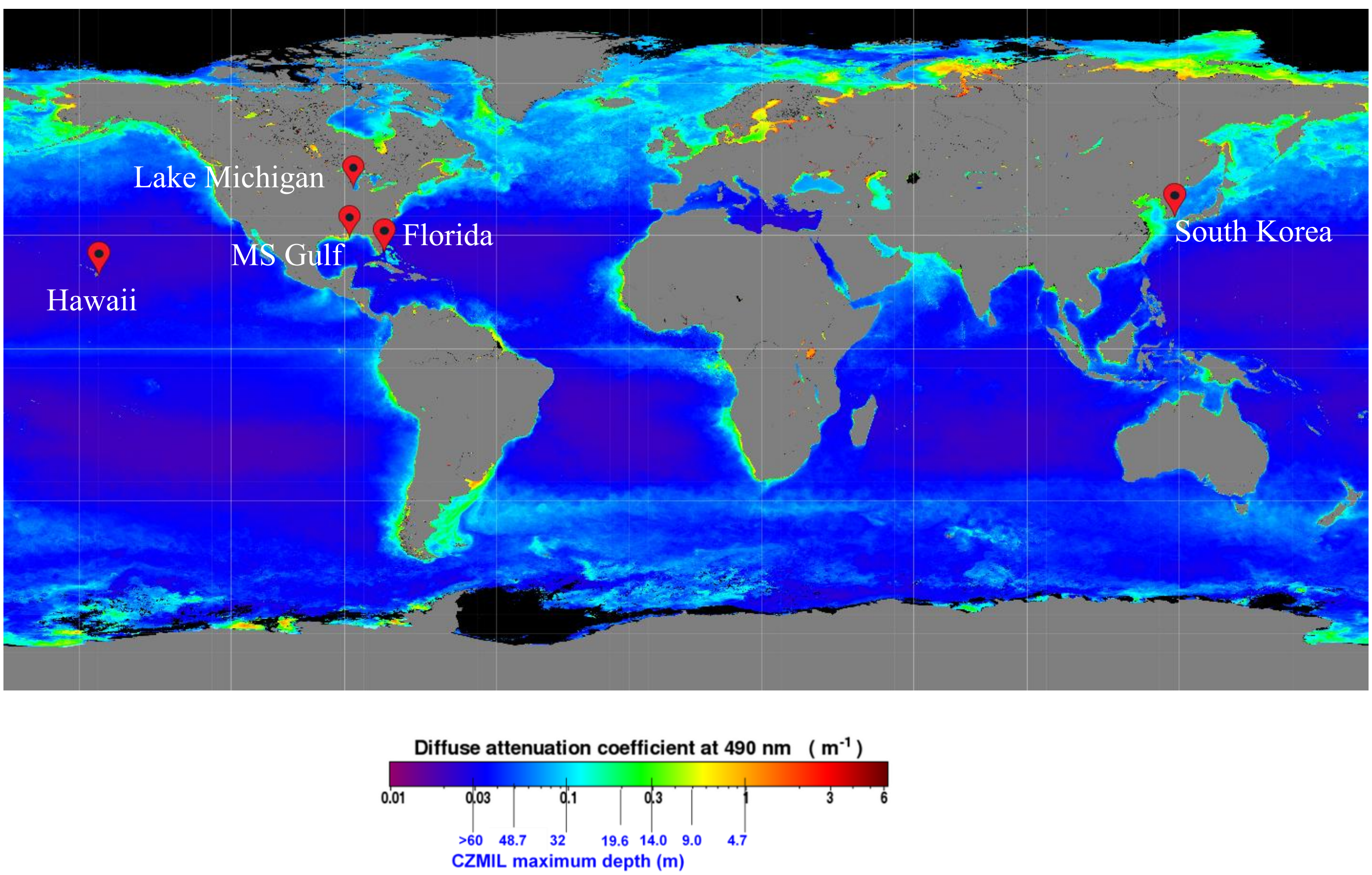

Fig. 4. Diffuse attenuation coefficient (K_d) map using Visible Infrared Imaging Radiometer Suite (VIIRS) 2014 composite data. Data source: [4]. Corresponding map of maximum CZMIL detectable depth is also shown in the color scale with the assumption of 15% bottom reflectivity.

II. COASTAL WATER CLARITY CHALLENGE

Airborne lidar systems (ALS) offer simultaneous and high-resolution mapping of bathymetry and adjacent topography. ALS deployment and coverage rates are more economical compared to ground-based types of mapping [5]. Lidar topo-bathy mapping systems have established themselves as the *de facto* tool for coastal management agencies to quantify and monitor near-shore regions.

The most challenging environmental factors that affect ALS are high water turbidity and low seafloor reflectance. There are two well-established procedures for characterizing the water turbidity used in the lidar bathymetric mapping community: 1) Secchi disk depth measurements expressed in meters and 2) the diffuse attenuation coefficient (K_d) expressed in meters inverse.

The Secchi disk is a traditional way of measuring water transparency that has been in use for well over a hundred years. In standard practice, the disk is lowered slowly into the water, and the depth at which it is no longer visible to the naked eye is called the Secchi depth [6]. There are several variations of the Secchi disk and we illustrate the two most commonly used types in Fig. 5. Secchi depth measurements are a good source of water turbidity measurements for all water bodies, including lakes and rivers, but they require ground personnel and are time consuming. Furthermore, reliable measurement requires the surveying personnel to follow strict standard measurement guidelines [6].

The optical properties of the incident light change in the water column due to the varied concentration of dissolved matter and suspended particles. In simple terms, K_d is a measure of the water column's optical properties as a function of depth at a given wavelength [7]. This parameter governs the amount of decay the incident laser pulse suffers as it propagates through the water column and this decay is exponential in nature. K_d is expressed in terms of m^{-1} [5].

Satellite-derived seasonal K_d maps are available online. They can be downloaded for use in planning surveys and serve as a good ALS bathymetric performance prediction tool in open ocean waters. The K_d map shown in Fig. 4 was generated using Visible Infrared Imaging Radiometer Suite (VIIRS) 2014 annual composite data. The maximum CZMIL-detectable depth for the corresponding K_d values are also marked below the color scale. The minimum pixel resolution of the publically available map is 250 m, meaning satellite-derived K_d products are applicable only for coastal or open ocean waters and are not practical for rivers and small lakes.

Maximum depth penetration for an ALS is directly proportional to the area of the receiver and the laser power. However, eye safety guidelines restrict the laser power used. It was shown in [8] that a wide-area aperture is key to improving depth penetration, but increasing the aperture diameter beyond 15 cm does not increase depth penetration significantly. Furthermore, aircraft structures have constraints on the port dimensions, limiting the area of the aperture.

Therefore the trade-offs inherent in the design of an ALS were carefully considered and the final system specifications optimized. CZMIL's specifications are listed in TABLE I.

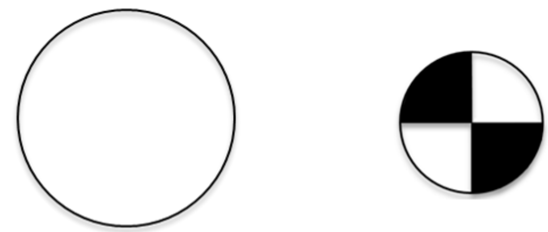

Fig. 5. Secchi disk types

Based on its pulse power and the area of its aperture it was shown in [9] that CZMIL has the highest single pulse figure of merit for bottom detection among all the ALS currently in operation.

The system performance coefficient K_dD_{max} is a metric used in airborne lidar hydrography to describe the maximum depth penetration capability of a bathymetric lidar for a given reflectance. TABLE II. lists typical K_d values for different water properties in terms of lidar bathymetric performance. CZMIL's K_dD_{max} value of 4.2 is valid for bottom reflectivity ≥ 15% and $0.07\ m^{-1} < K_d < 0.4\ m^{-1}$. However, it is important to note that it is not possible to accurately predict the maximum depth measurement of an ALS if bottom reflectance is less than 5% or if K_d measurements are outside the above valid range.

TABLE II. DIFFERENT WATER TYPES

Water Type	Typical Examples	K_d Values
Clear	Hawaii, Bahamas, Florida east coast	$< 0.08\ m^{-1}$
Moderately clear	Florida west coast, East coast of South Korea	$0.08 – 0.2\ m^{-1}$
Turbid	Sea of Japan coast	$0.2 – 0.4\ m^{-1}$
Very turbid	Mississippi Gulf, East China Sea	$> 0.4\ m^{-1}$

III. CZMIL PERFORMANCE IN DIFFERENT COASTAL ZONES

In the following section we discuss CZMIL's bathymetric performance in the different water types listed in TABLE II. We also discuss typical challenges encountered in processing coastal lidar data and how they are resolved using examples.

A. Clear waters (Florida, Hawaii)

The South Florida Ocean Measurement Center (SFOMC) off the coast of Ft. Lauderdale is a comprehensive bathymetric test facility. JALBTCX uses this facility for periodic calibration and validation of CZMIL systems. The CZMIL data discussed here were successfully acquired on May 4-8 2012 and again on July 23-26 2014 for this purpose.

JALBTCX used a CZMIL system to survey the Hawaiian Islands in October 2013. The diffuse attenuation coefficient was approximately $0.06\ m^{-1}$ around the islands. In Fig. 6 we show the K_d map at 532 nm in October 2013 over Kauai, Hawaii. This was part of a production survey and covered over 1000 km of shoreline. The collection effort extended 300 m inland and 1000 m offshore.

1) Seamless topo-bathy maps

Lidar waveforms are time-resolved, and the estimation of depth and other environmental products requires temporal separation between surface and bottom returns. Due to the hardware limitations of the previous generation of systems, surface and bottom returns were not resolved. This is clearly evident in the comparative plots in Fig. 7. Consequently, depth measurements are challenging in very shallow water. On the other hand, CZMIL's waveform offers a clear distinction between the surface and bottom returns.

CZMIL's 7 segmented shallow channels and a short laser pulse (2.2 ns) provide better than 1-m horizontal and vertical spatial resolution over land and shallow waters. To meet the requirements of client-driven applications (such as shoreline positioning) we have also developed a semi-analytical procedure to estimate depths in shallow water. CZMIL's hardware innovations combined with advanced data processing techniques enable the generation of seamless topo-bathy maps (see Fig. 8) [1], [10].

2) Small object detection capability

The delineation of navigational hazards is a critical aspect of nautical surveying. International Hydrographic Organization

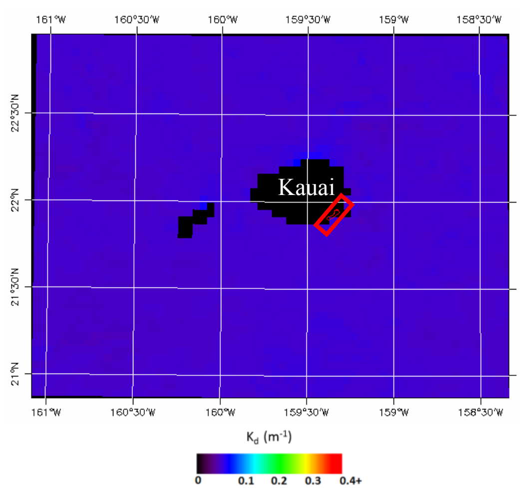

Fig. 6. Diffuse attenuation Coefficient (K_d) map with at 532 nm, based on Aqua MODIS data from October 2013 off the coast of Kauai, Hawaii (survey location marked).

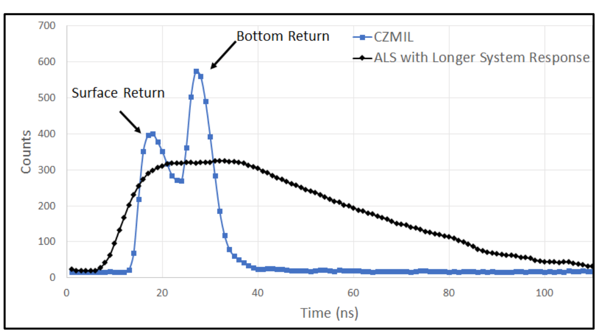

Fig. 7. Comparison of waveforms from CZMIL and an ALS with longer system response time (3.7 ns for CZMIL as opposed to 12 ns for the ALS) off the shallow waters of Ft. Lauderdale, FL at a depth of 1.5 m.

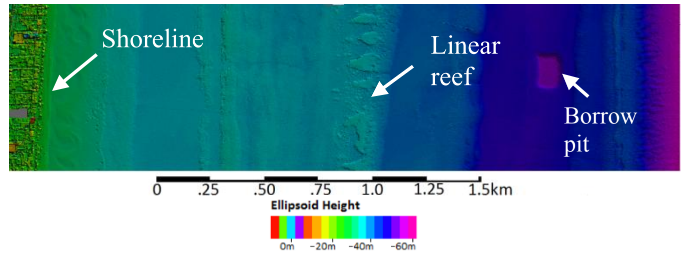

Fig. 8. Seamless topo-bathy DEM generated from CZMIL data off the coast of Ft. Lauderdale. Some of the seafloor features are marked on the image.

(IHO) standard 1a requires the detection of an "object (cubic features >2 meters) in depths up to 40 m"[11].

A detailed analysis of CZMIL's object-detection capability and validation is reported in [12] and [13]. The survey area over SFOMC contains several known areas with small objects on the seafloor. Here we discuss one such area containing small objects. Fig. 9a is the multi-beam sonar data showing these objects arranged in a row at a depth of approximately 12 m. The objects are conical with approximately 1-m base and 1-m height. The multi-beam data were collected by University of Southern Mississippi (USM) as part of the CZMIL system validation efforts. CZMIL data were collected on May 4-8 2015 and the multi-beam data collected on May 9-15, 2012. In Fig. 9b all 12 conical objects can be separately identified in the CZMIL data. We also show CZMIL waveform return with the secondary return from one of these objects in Fig. 9c.

It was shown in [14] that D_{index} is a better discriminability index metric than the Signal-to-Noise ratio for optical signals due to the following:

a. Noise distribution is a function of the signal.

b. Noise distribution is not normal.

c. D_{index} is a measure of distinguishability between two probability distributions, A and B, for the random quantities at the detector output in the absence (A) and in the presence (B) of the signal to be detected [15]:

$$D_{index} = \left| i_B - i_A \right| / \left(S_A - S_B \right)^{1/2} \quad (1)$$

where i_A and $\boldsymbol{i_B}$ are the mean values for distributions A and B, respectively. S_A and S_B are the corresponding standard deviations.

We employ classic signal detection theory when detecting returns from lidar waveforms. For every lidar waveform, we determine the noise and (using the peak power of the detected return) we calculate the probability of detection (P_d) for a given false alarm probability. The relationship between D_{index} and P_d is given by:

$$\mathrm{P}_d = \tfrac{1}{2} Erfc\left[Erfc^{-1}(2\mathrm{P}_f) - D_{index} \right] \quad (2)$$

where P_f is the false alarm probability and *Erfc* is the error function. CZMIL's P_d as a function of depth for different water types is illustrated in Fig. 10 for P_f = 1e-5.

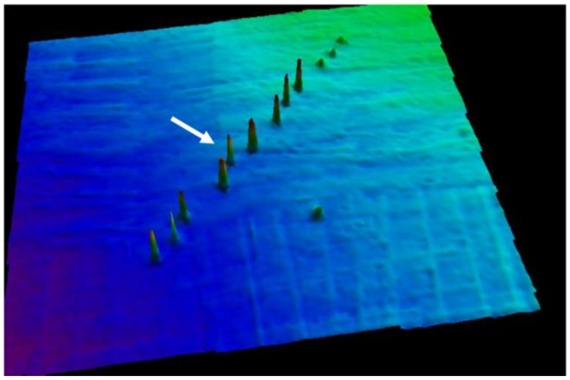

(a) SFOMC objects located in multi-beam sonar data. The objects are conical with approximately 1-m base and 1-m height at 12 m depth.

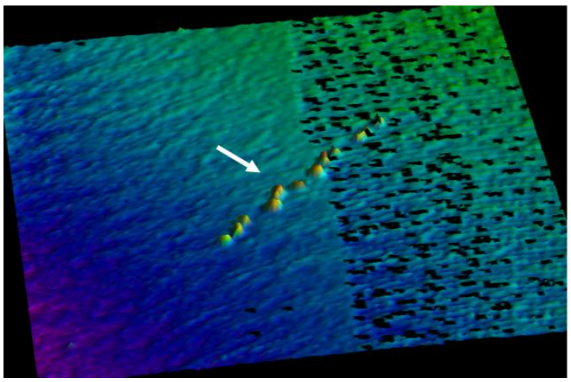

(b) SFOMC objects located in CZMIL data.

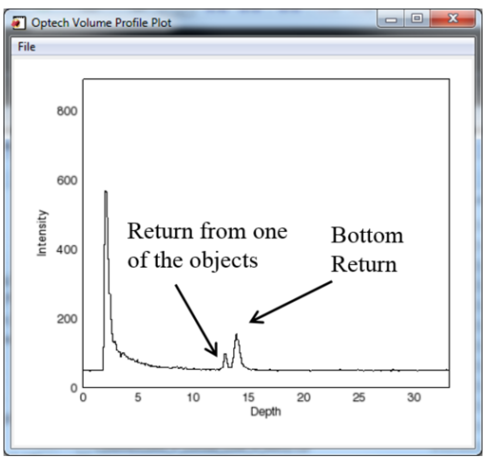

(c) CZMIL shallow channel waveform return from one of the objects.

Fig. 9. Illustration of CZMIL's small object detection capability

HydroFusion adopts a heuristic approach to interest point detection algorithms in its data processing by incorporating spatial information. This further enhances detection capability by keeping the false alarm rate low, particularly in deeper waters when the signal return is low. An example of automatic detection of low signal level returns in deep water is illustrated in Fig. 11.

3) Robust surface detection

To accurately report depths, it is critical to correctly determine the air/water interface. Several environmental factors

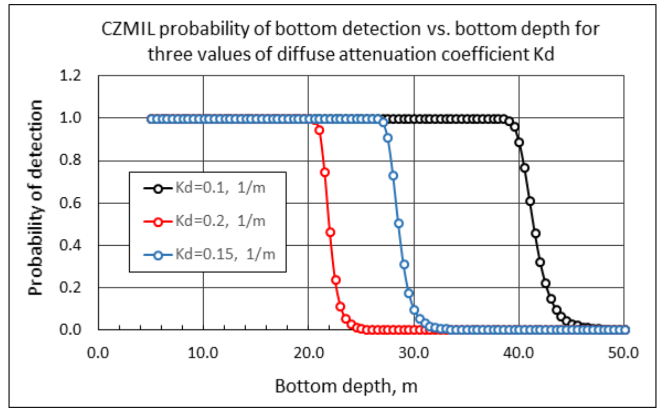

Fig. 10. CZMIL P_d as a function of depth for different water types.

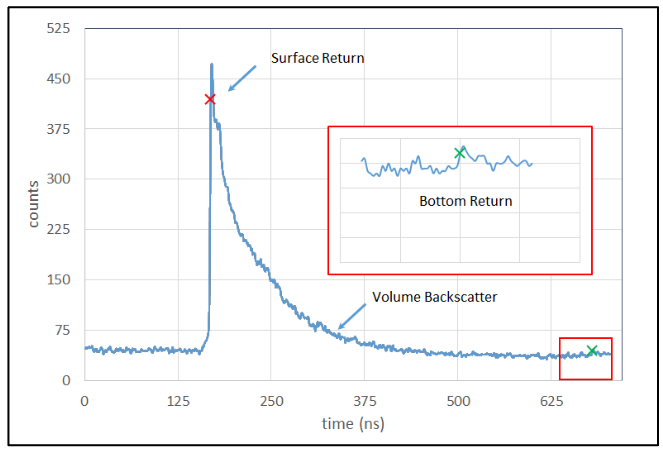

Fig. 11. Typical bathymetric waveform in clear and deep water with bottom return at 55 m.

can perturb the inflection point locations on the surface return. Areas of breakwater can result in "sea sprays" or "sea smoke" that in turn can result in returns much earlier than the actual sea surface return. This leads to inaccurate depth measurement. HydroFusion has special surface detection algorithms to discriminate against these types of returns.

Surface waves combined with CZMIL's short laser pulse can result in "merged" surface returns consequently leading to multiple detection points in CZMIL's shallow channels. All surface detection points are subjected to quality checks to determine the optimum surface location times and accurately segment the lengths of the in-air and in-water optical paths. Surf zones are common in areas like Hawaii's coastal zones and can result in "white water" where ALS has difficulty penetrating the water column. CZMIL mitigates this to a certain extent since it utilizes a circular scanner and therefore offers two independent looks through the surf zone.

The K_d at 532 nm from Aqua MODIS data for October 2013 was less than 0.06 m^{-1} around Hawaii. Off the island of Kauai, depths were detected to 58 m (see Fig. 12) while depths to 65 m were seen off the Big Island of Hawaii. Florida waters were not as clear. The K_d values ranged from 0.08-0.10 m^{-1} during the survey. CZMIL achieved bathymetry to a depth of 43 m on both surveys over the Florida waters.

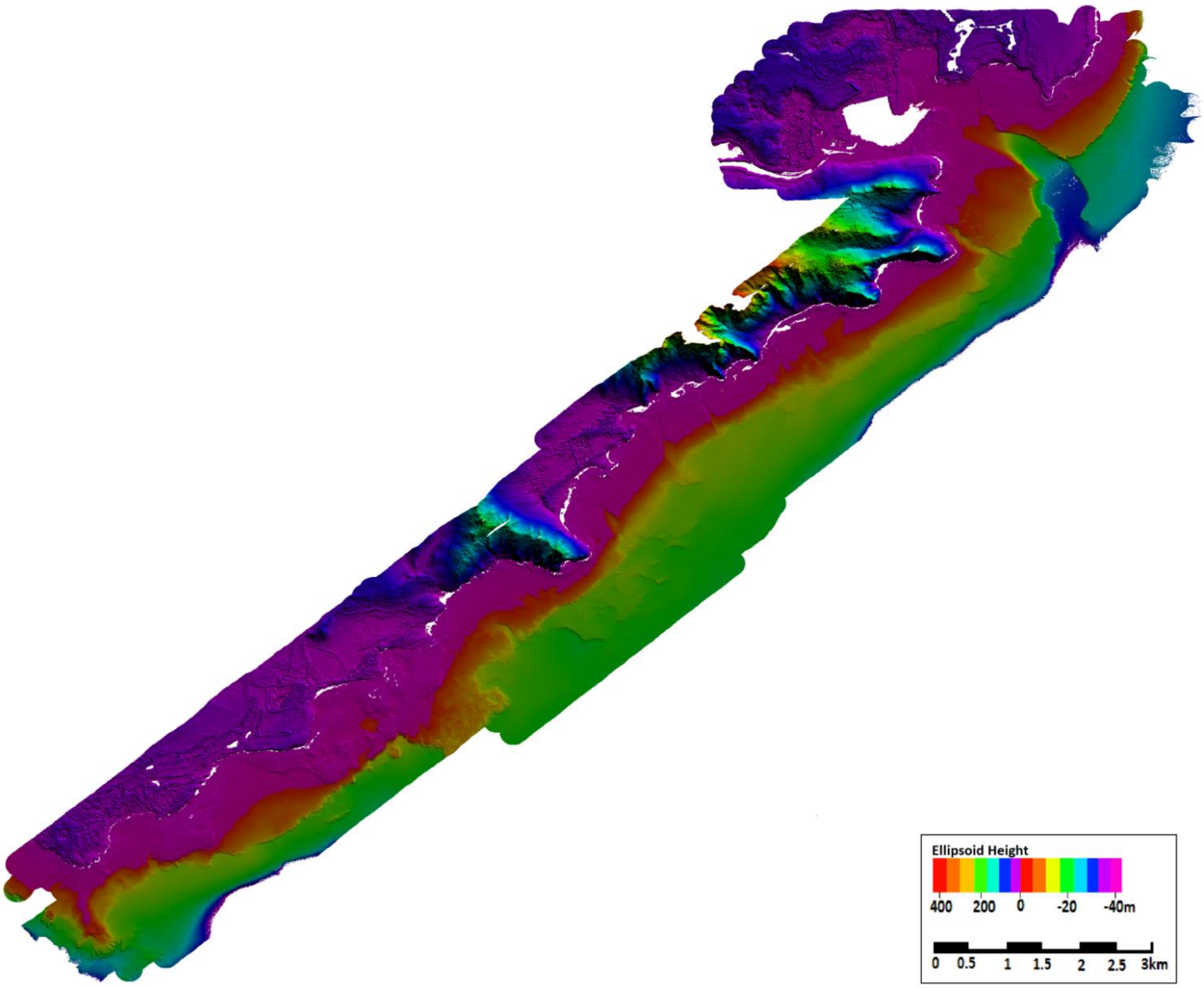

Fig. 12. Topo-bathy DEM generated from CZMIL data off the coast of Kauai, Hawaii.

B. Moderately clear waters (East coast of South Korea)

Over multiple missions in South Korea between 2013 and 2015 CZMIL Nova surveyed more than 2000 km² on the east and west coasts as well as the island of Jeju to the south. CZMIL was installed on a King Air E-90 for the Korean Hydrographic and Oceanographic Administration (KHOA).

The west coast of South Korea presents a big challenge to data collection as the water quality ($K_d > 0.3$ m^{-1}) is very poor (see Fig. 13). Jeju Island and the east coast offer moderately cleaner waters, but with drastic changes in terrain, some of which require a higher flying altitude during collection.

Here we show survey results from one of the survey areas on the east coast of South Korea near Donghae. Here the waters are moderately clear. The K_d value for this area from the Aqua MODIS K_d map in Fig. 13 is approximately 0.10-0.20 m^{-1}. The maximum depth detected along the coast was about 30 m (Fig. 14a). The maximum depth detectable matches the K_dD_{max} specification for CZMIL.

C. Turbid waters (Near-shore regions, Lake Michigan)

In August 2012, JALBTCX used a CZMIL system to survey in the Great Lakes region as part of the National Coast Mapping Program (NCMP). Here we focus on Calumet Harbor on Lake Michigan. The area of interest is approximately 35 km² and contains mostly turbid water with a K_d near 0.20 m^{-1} (see Fig. 15).

A lidar return signal attenuates with depth and is a function of water turbidity and can be described as $e^{-2K_{sys}\cdot depth}$, where K_{sys} is the lidar system attenuation coefficient. K_{sys} is a function of water inherent optical properties, lidar transmitted beam divergence (*DIV*), receiver optical system field-of view (*FOV*) and altitude. Note that for the situation (a), when $FOV \approx DIV$, K_{sys} is near c – the beam attenuation coefficient and for (b), FOV >> DIV, $K_{sys} \approx K_d$. The case (b) is corresponds to the CZMIL Deep channel.

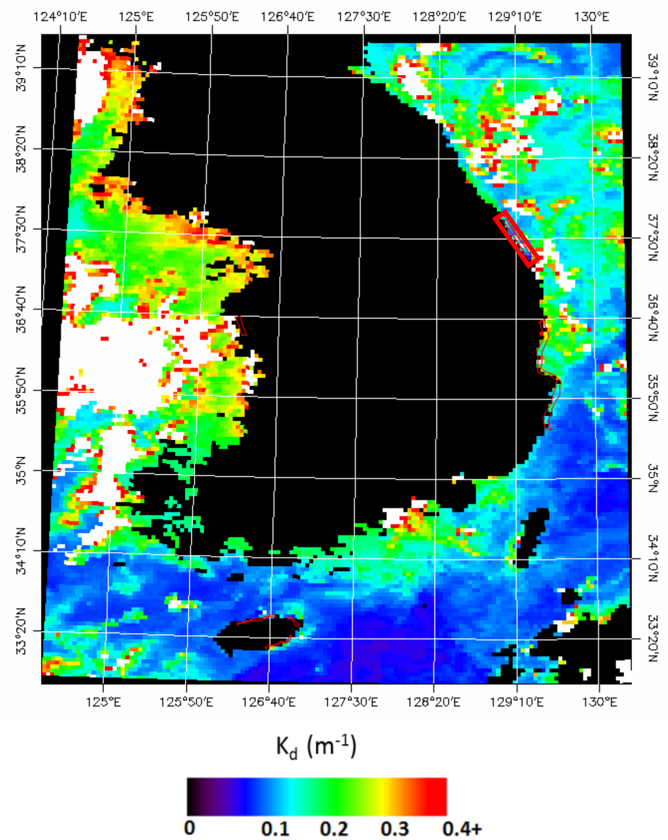

Fig. 13. Diffuse attenuation coefficient (K_d) map of South Korea at 532 nm using Aqua MODIS data from September 2013 (Donghae coast marked).

The bottom return signal attenuation is more pronounced in turbid water conditions. We have incorporated a Turbid Water Module (TWM) in the data processing workflow specifically designed to detect and extract bathymetry measurements from turbid waters and muddy, less-reflective seafloors. Fig. 16 illustrates an example of the module's detection capability.

Most of Lake Michigan (Fig. 15) is moderately clear, but the near-shore regions where the survey was conducted are turbid. Furthermore, some near-shore areas have increased turbidity due to river flow and industrial activity in the watershed area and the lakebed could not be mapped by CZMIL. In the survey areas where K_d values were greater than 0.25 m^{-1}, CZMIL achieved bathymetry to a depth of approximately 12 m (see Fig. 17).

D Very turbid waters (Mississippi Gulf, Peace River, Florida)

CZMIL successfully acquired data over Cat Island, approximately 13 km offshore from Mississippi, on April 25, 2012. This survey was part of the system validation tests [12]. The diffuse attenuation coefficient (K_d) at 531 nm from Aqua MODIS data on April 24, 2012 was from 0.3 to 0.8 m^{-1} around Cat Island (see Fig. 18). At the same time of CZMIL's flight over Cat Island, the USM field data collection team acquired Secchi depth measurements and optical properties as well as acoustic data. The Secchi depth observations ranged from 1.3 m to 3.1 m.

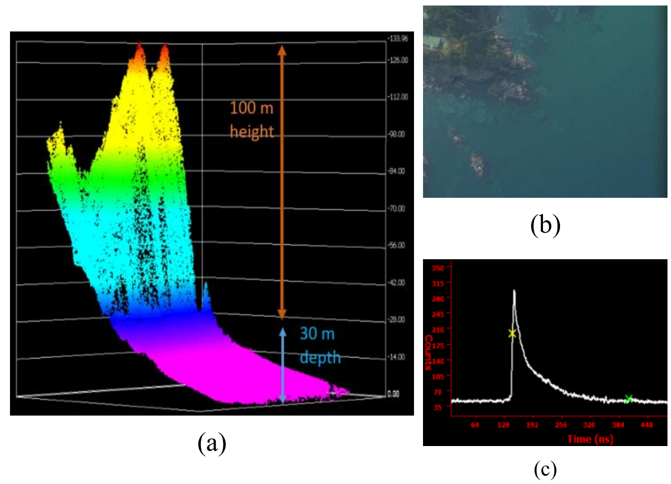

Fig. 14. (a) CZMIL point cloud from Donghae area, South Korea collected in September 2013. (b) T-4800i camera image of the same area. (c) A waveform extracted from the deeper part of the survey area.

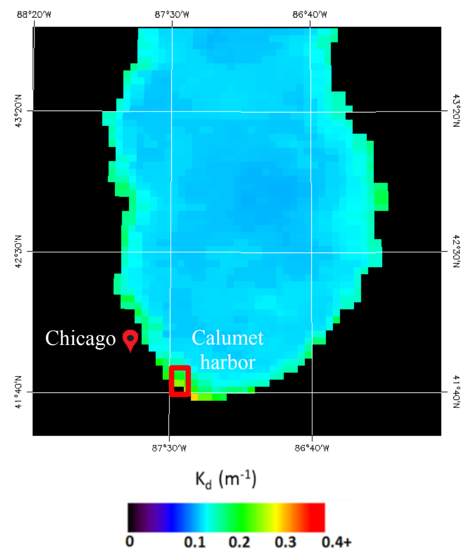

Fig. 15. Diffuse attenuation coefficient (K_d) map at 532 nm using Aqua MODIS data from August 2012 of Lake Michigan (area of interest marked).

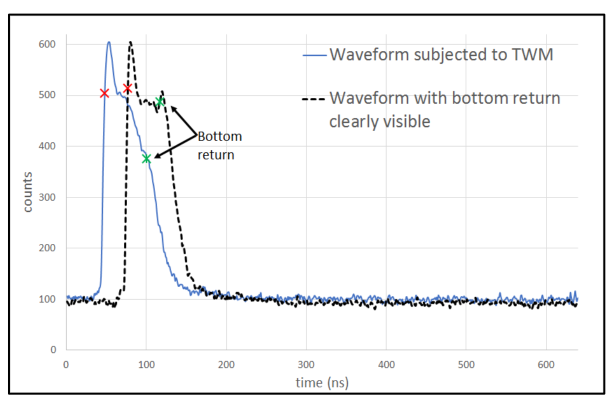

Fig. 16. Advanced signal processing techniques are used to detect low signal level bottom returns as a result of turbid waters and low-reflectance seafloors.

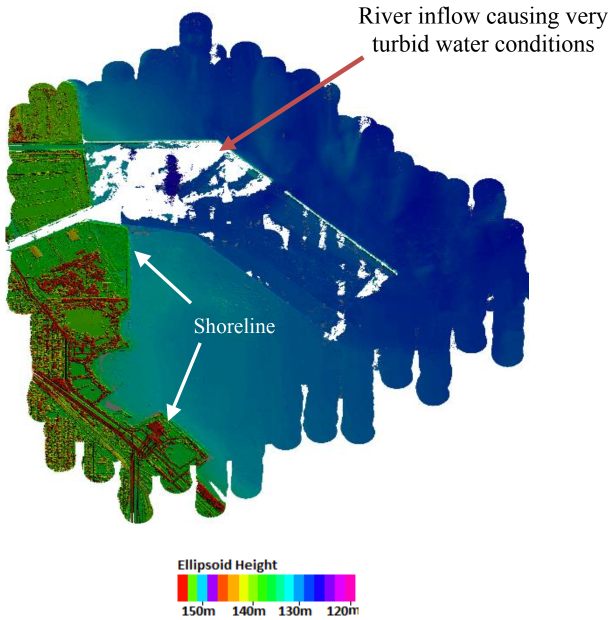

Fig. 17. CZMIL DEM in turbid water conditions over Calumet Harbor in Lake Michigan.

These observations, when converted to the corresponding K_d values, confirm the satellite-based K_d observations. The maximum achieved bathymetry from CZMIL on the east side of the island was to a depth of 9 m and the K_d values are in the 0.3-0.4 m^{-1} range.

Through the CZMIL Project Program a preliminary test project was conducted in collaboration with Dewberry for South West Florida Water Management District (SWFWMD). In this pilot test project, Tampa Bay, Florida and Peace River, south of the Bay were surveyed. This was a small survey covering an area of 12 km^2. Secchi depth measurements were taken along the river by SWFWMD and the values were observed to be less than 1 m. These observations combined with visual images (Fig. 19a) illustrate the water turbidity. Due to biological activity in the river we assume bottom reflectance is close to 5%. All these factors make it challenging for the lidar to detect the river bed. Nevertheless, CZMIL was able to detect river bed in some sections of the river and we show preliminary results in Fig. 19 a, b and c.

IV. Conclusion

We discussed CZMIL's bathymetric performance across a broad spectrum of littoral zones. The maximum depth detected is consistent with the predicted system performance coefficient.

Satellite-derived K_d maps and Secchi depths are valuable survey planning tools that gives us the seasonal understanding of water turbidity but have some limitations. Therefore in-depth understanding of these parameters in relation to the system performance coefficient is necessary for the maximum utilization and validation of an ALS.

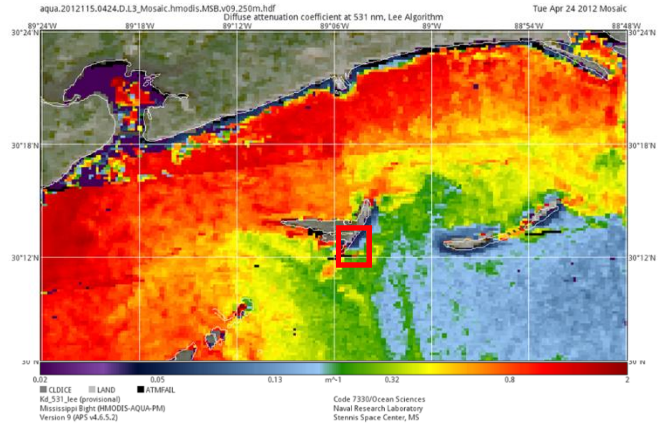

Fig. 18. Diffuse attenuation coefficient map with 250-m resolution at 531 nm using Aqua MODIS data from April 24, 2012 of Cat Island, Mississippi (survey location marked).

(a) Camera Image of a section of Peace River.

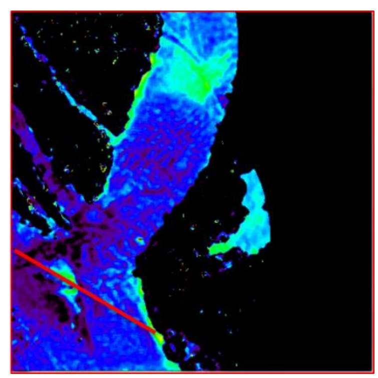

(b) Lidar DEM of the corresponding area.

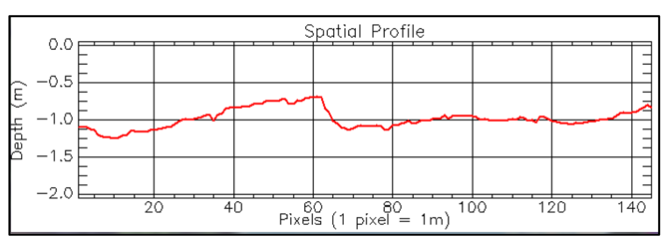

(c) Depth profile across the transect.

Fig. 19. Peace River, Floida

Acknowledgment

The Coastal Zone Mapping and Imaging Lidar (CZMIL) program was supported by the U.S. Army Corps of Engineers under contract W912HZ-06-C-0048. Thanks to JALBTCX for continued support through the CZMIL Improvement program.

We would like to thank the following agencies for providing us with CZMIL data: JALBTCX, for data collected in Florida, Lake Michigan, Hawaii, and Mississippi Gulf; Korea Hydrographic and Oceanographic Administration (KHOA) and GeoMonitoring Inc. for the data collected in South Korea.

We would also like to acknowledge South Florida Ocean Measurement Center (SFOMC) for providing seafloor target data in Fort Lauderdale, Florida and thank the Naval Research Lab (NRL) Stennis Space Center for providing Aqua MODIS K_d maps.

References

[1] Tuell, G.; Barbor, K; Wozencraft J., "Overview of the coastal zone mapping and imaging lidar (CZMIL): a new multisensor airborne mapping system for the U.S. Army Corps of Engineers," Proc. SPIE, 7695 (2010).

[2] Wozencraft J. M., "Requirements for the Coastal Zone Mapping and Imaging Lidar (CZMIL)," Proc. SPIE 7695 (2010), DOI: 10.1117/12.851891.

[3] Teledyne Optech website, http://www.teledyneoptech.com/wp-content/uploads/CZMIL-Project-Program-140822-WEB.pdf, accessed 08 August 2015.

[4] NASA's OceanColor Web database, http://oceancolor.gsfc.nasa.gov/cgi/l3, accessed 08 August 2015.

[5] Gary C. Guenther, A. Grant Cunningham, Paul E. LaRocque, and David J. Reid, "Meeting the Accuracy Challenge in Airborne Lidar Bathymetry," Proceedings of EARSeL-SIG-Workshop LIDAR Dresden/FRG June 16,17 2000.

[6] Environmental Protection Agency's "Standard Operating Procedure for Zooplankton Sample Collection and Preservation and Secchi Depth Measurement Field Procedures", www.epa.gov/greatlakes/monitoring/sop/chapter_4/LG402.pdf, accessed 30 September 2014.

[7] Martin A. Montes,1, James Churnside, Zhongping Lee, Richard Gould,Robert Arnone and Alan Weidemann, "Relationships between water attenuation coefficients derived from active and passive remote sensing: A case study from two coastal environments," Applied Optics. 38, 2990–9 June 2011.

[8] Fuchs E., and Tuell, G.H., "Conceptual Design of the CZMIL Data Acquisition System (DAS): Integrating a New Bathymetric Lidar with a Commercial Spectrometer and Metric Camera for Coastal Mapping Applications," Proc. SPIE, 7695 (2010).

[9] Wayne Wright, Nicholas Johnson, "National Coastal Mapping Strategy - Bathymetric Lidar Quality Levels Introduction and Discussion", 15th Annual JALBTCX Airborne Coastal Mapping and Charting Workshop, Corvallis, OR, June 16-18, http://shoals.sam.usace.army.mil/Workshop_Files/2014/Day2_pdf/1500_Wright.pdf

[10] Aitken, J., Ramnath, V., Feygels, V., Mathur, A., Kim, M., Park, J.Y., Tuell, G.H., "Prelude to CZMIL: Seafloor Imaging and Classification Results Achieved with CHARTS and the Rapid Environmental Assessment (REA) Processor", Proc. SPIE 7695 (2010).

[11] IHO Standards For Hydrographic Survey, Special Publication No. 44, International Hydrographic Bureau, Feb. 2008, 5 ed. 28 pp.

[12] Dodd, D., "CZMIL Validation Survey: Comparison with Acoustic Data Vertical Component, Fort Lauderdale," Report by the Hydrographic Science Research Center at University of Southern Mississippi. Prepared for JALBTCX and Optech, Inc., 2012.

[13] Barbor, K., Dodd, D., "CZMIL Validation Report: Horizontal and Vertical Accuracy Assessment of CZMIL Sensor Data," Report by the Hydrographic Science Research Center at University of Southern Mississippi. Prepared for JALBTCX and Optech, Inc., 2012.

[14] Sakett B. Indices of Discriminability, Nature, v.241, 133-134, 1973.

[15] Egan J.P. Signal Detection Theory and ROC Analysis, Academic Press, NY, 1975.